

Integrated optical microcavity infiltrated by liquid crystals for CWDM applications

F. RIBOLI^{1,*}, N. DALDOSSO¹, M. MELCHIORRI¹, G. PUCKER²,
C. KOMPOCHOLIS², A. LUI², AND L. PAVESI¹

¹*Department of Physics, University of Trento, via Sommarive 14, 38050 Povo-Trento, Italy*

²*ITC-IRST, Microsystems Division, via Sommarive 18, 38050 Povo-Trento, Italy*

(*author for correspondence: E-mail: riboli@science.unitn.it)

Received 7 October 2005; accepted 31 January 2006

Abstract. A Fabry-Perot optical microcavity based on liquid crystal infiltration integrated in a waveguide has been designed and fabricated. Careful optimization of the cavity geometry allows designing a device with a simulated resonance peak transmission of 95% with a linewidth of about 1.7 nm. Based on this simulation, a first prototype has been fabricated and tested.

Key words: CMOS integrated circuits, Fabry-Perot resonators, liquid crystals, optical switches, waveguides

1. Introduction

Various silicon compatible photonic devices have been studied and realized in this last decade (Pavesi and Lockwood 2004). Among these, one important function is the routing of optical signals among different channels. The best option for a router is a reconfigurable optical one for which the routing is dynamically addressed. The key component of an optical router is the optical switch, which transmits or blocks the optical signal depending on the routing protocol. Optical switches can be done either by using moving mirrors or by exploiting the wavelength dependence of optical filters. Also for the optical switch, the aim is reconfigurable switching. In Riboli *et al.* (2005) we have proposed a new architecture of an integrated Fabry-Perot (FP) microcavity. The aim of that work was to propose and theoretically characterize a new architecture of a FP microcavity integrated on silicon on insulator (SOI) waveguide. Particular care in the design was paid to the feasibility of the resulting scheme within silicon foundries.

In this work, we show the preliminary experimental results about the realization of the device proposed in Riboli *et al.* (2005). The device has been realized starting from a Si₃N₄ multilayer waveguide (Melchiorri *et al.* 2005) instead of a SOI waveguide, due to the availability of the technology.

In the first part, we briefly show the architecture of the device describing the role of the design parameters. In the second part, we show the architecture of the realized device with a description of the fabrication process. The last part will be devoted to a preliminary test of the realized device and to the comparison of the simulation results with the measured ones.

Although a detailed comparison with existing switches for optical signal routine is premature, the proposed device has some interesting peculiarities: it does not have moveable parts like in MEMS switches, it is very small (less than $10\ \mu\text{m}$) and the switching speed and the wavelength of operation can be adjusted by using different materials and different physical effects.

2. Design and optimization of the SOI based device

The device is based on a FP resonator integrated along a channel waveguide and composed by two symmetric Distributed Bragg Reflectors (DBRs) separated by an empty space (cavity). In the simulation, each DBR is formed by three repetitions of Si-SiO₂ $\lambda/2$ -thick stacks. The cavity is a λ -thick cavity which can be filled by a suitable medium to achieve tunability. In our experiments the cavity is filled with liquid crystals (LC) to allow an electrical control of their refractive index. In the simulation, LC are simulated by an effective refractive index inserted into the cavity. Furthermore, we assume the optical axis of LC perpendicular to the propagation direction of light and an orientation of the LC so that the transverse electric (TE) polarized mode is parallel to the extraordinary ray in the cavity. The electro-optic behavior of the LC is simply simulated by changing the refractive index value.

The channel waveguide, where the FP is integrated, is a silicon waveguide, $5\ \mu\text{m}$ thick, clad by SiO₂. The bottom SiO₂ cladding is $3\ \mu\text{m}$ thick to guarantee isolation from the Si substrate while the thickness of the top SiO₂ cladding is an optimization parameter. The cross section of the proposed device is shown in Fig. 1a.

The architecture of the device is particularly suitable to be simulated with the eigenmode expansion (EME) method (Sudbo 1993a, b). The EME method is a bi-directional propagation method that solves exactly the Maxwell equations. This method is particularly suited for those structures that can be viewed as a series of slices with invariant refractive index profile along the direction of propagation of light that is just the case of the device shown in Fig. 1a. The method accuracy depends on the number of enabled eigenmodes in each slice. We have used a commercial software to perform the simulations.¹ In the simulation, the device is represented by 17

¹Photon Design Software: FimmWave and FimmProp version 4.1.

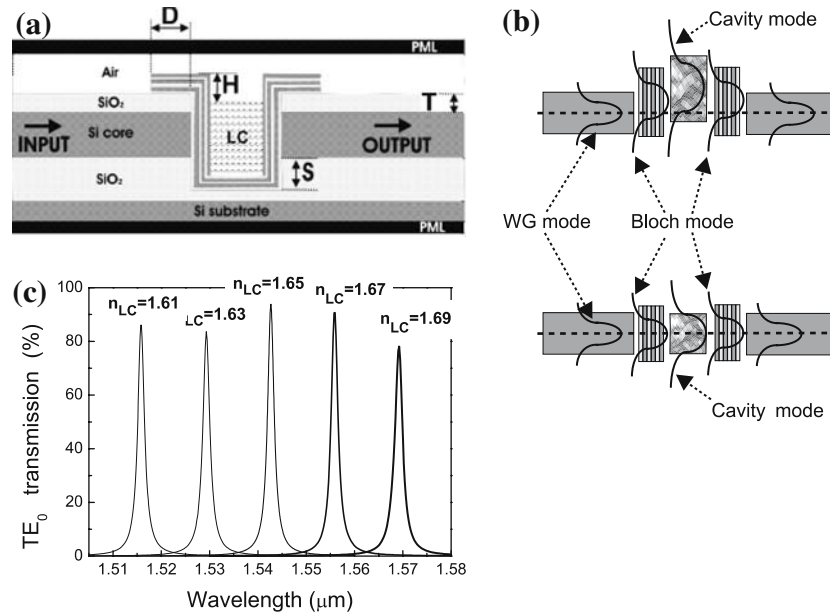


Fig. 1. (a) Cross-section of the proposed device. The various parameters, optimized in the simulations, are D , H , T , S and are defined in the text. (b) Sketch of the various optical modes in our device: (upper plot) mismatched case (lower plot) matched case. (c) TE transmission spectrum for various values of the refractive index of the LC, n_{LC} . Such variation corresponds to a bias of few volts when the E7 LCs are used. The optimised device has $S = 1 \mu\text{m}$, $T = 0 \mu\text{m}$, $D = 23.2 \mu\text{m}$, and $H = 1.5 \mu\text{m}$.

different slices, of which only nine are independent; about 120 eigenmodes are enabled in each slice. With this number of modes we estimate an error of 0.5–1% on the transmission values due to the finite basis set. The whole numerical characterization has been performed by using the effective-index method.

The target of the optimisation is to maximize the resonant peak transmission intensity of the fundamental waveguide mode from the input to the output waveguide, i.e., to reduce the insertion losses of the switch.

The input planar waveguide supports about 30 guided modes. In the simulation, we excite only the fundamental mode of the input waveguide and we perform a wavelength scan around the resonance wavelength and record the fundamental mode intensity in the output waveguide. The maximization of the resonant peak transmission value can be viewed as the maximization of the modal matching among the eigenmodes in each slice. All the radiating modes, produced during the multiple reflections in the cavity, are absorbed by the PML (perfectly matched layer) layers without influencing the spectrum of the fundamental mode.

The performance of the device (minimization of the insertion losses) has been optimized varying four parameters, namely S , T , D , H : S is the depth

of the cavity in the bottom cladding, T is the thickness of the top cladding, D is the length of the DBR layers which overcoat the top cladding, and H is the thickness of the cavity without the LC. By variation of the S , T and H parameters, it is possible to optimize the matching among the fundamental TE_0 mode of the waveguide, the Bloch mode of the DBR and the resonant mode of the LC filled cavity (Ctyroky 2001; Palamaru and Lalanne 2001). Figure 1b shows schematically the mismatched case (upper plot) and the optimized case (lower plot) where the mode profiles of each fundamental mode (waveguide mode, Bloch mode and cavity mode) are matched to reduce the insertion losses.

The D parameter has a different role, influencing the coupling between the cavity and the resonant structure formed by the multilayers over the top cladding. This last resonant structure arises due to light reflections at the end facet of the multilayers.

The optimization has been made with a LC refractive index $n_{LC} = 1.65$, which is suitable for typical liquid crystals.² Optimum parameters turn out to be $H = 1.5 \mu\text{m}$, $S = 1 \mu\text{m}$, $T = 0 \mu\text{m}$ and $D = 23.2 \mu\text{m}$ which gave a quality factor of 900 and an insertion loss of less than 0.2 dB. It is worth noting that no contribution due to the liquid crystal absorption has been taken into account for this first optimization. Once the structure is optimized, n_{LC} was varied to simulate the effects of an external electric field applied to the LC. Figure 1c shows the transmission spectra of the optimized device, for various n_{LC} . A resonant peak shift of 55 nm is observed when the refractive index of the LCs is varied from 1.61 to 1.69. This range of variation is practically achievable (Pucker *et al.* 2004). Despite some variations in the maximum transmission can be observed, its value is never lower than 78% (maximum insertion losses of 1.1 dB) with a spectral width of 1.7 nm ($Q = 900$).

3. Realization of the Si_3N_4 based device

The basic assumptions of this device (tunable FP) have been previously demonstrated in a system realized by two DBR mirrors bonded together (Pucker *et al.* 2004): a resonance shift of 100 nm by increasing the bias from 4 to 10 V was observed with a typical switching time of 5 ms (Mezzetti *et al.* 2004). In this work we report our efforts to integrate a FP structure in a channel waveguide and characterize its insertion loss when LCs are filled in the cavity. Due to the availability of the process and contrary to the simulations we used Si_3N_4 as waveguide core materials.

²This value has been chosen because of the large availability of liquid crystals with refractive index between 1.6 and 1.7. For example E7 has $n_e = 1.75$ and $n_o = 1.523$.

The fabrication uses standard CMOS technology and processes. The only material which is not standard in CMOS processing is the LC. For this reason we filled the cavity with LC as a back-end process. Briefly the fabrication process was the following. It starts with the growth of a $1.5\ \mu\text{m}$ thick thermal oxide layer on 4 inch silicon wafers; then a $1\ \mu\text{m}$ thick SiO_2 layer (low pressure chemical vapor deposition (LPCVD), precursor: tetra-ethyl-orthosilicate) is deposited. This $2.5\ \mu\text{m}$ thick oxide layer formed the buffer layer on which Si_3N_4 multilayer waveguides were deposited (see (Daldosso *et al.* 2004) for details). Since LPCVD Si_3N_4 adds high tensile stress, which can cause fracture of the deposited films, the waveguide deposition is interrupted after some layers and the Si_3N_4 layers are removed on the whole wafer except the regions where the waveguides are situated. Then the remaining SiO_2 and Si_3N_4 layers are deposited to form the planar waveguides. Waveguides of widths ranging from 3.5 to $13\ \mu\text{m}$ are formed by photolithographic processes and plasma etching. On top of the waveguides, a 0.5 or $1\ \mu\text{m}$ thick LPCVD oxide is deposited as cladding layer. At this point, a trench is etched perpendicular to the waveguides with a dedicated plasma-etching process. The trench defines the place along the rib-waveguide where the FP will be fabricated. The process is optimized to have same Si_3N_4 and SiO_2 etch rates which should yield perpendicular sidewalls with low roughness. The nominal width of the trenches was ranging from 2.8 to $5.2\ \mu\text{m}$. By using conformal growth DBRs are deposited by LPCVD. The DBRs have 3 periods of Si ($100\ \text{nm}$)/ SiO_2 ($270\ \text{nm}$) $\lambda/4$ stacks. Scanning electron microscopy (SEM) analysis show that the LPCVD deposited layers are very conformal and the layer thickness is constant on the wafer surface and within the trenches. Subsequently, the DBRs are removed by plasma etching everywhere on the wafer except a $23\ \mu\text{m}$ thick region across the trenches. A SEM image of a cross-section of the obtained structure is given in Fig. 2.

The facets of the waveguides were prepared by a process described in detail in (Daldosso *et al.* 2004). The wafers were diced to chips of approximately $2 \times 3\ \text{cm}$ where each chip contained waveguides with the whole range of channel-widths from 1.5 to $13\ \mu\text{m}$ with integrated the Fabry-Perot plus a series of reference waveguides.

4. Preliminary experimental results

Transmission measurements were used to characterize integrated FP. Light from a tunable laser (1260 – $1550\ \text{nm}$, $2\ \text{mW}$) through a single mode polarization maintaining tapered fiber, mounted on a nano-positioning system, was coupled into the waveguide by using the butt coupling method. Two linear polarizers and a half-wave plate were used to polarize the laser light.

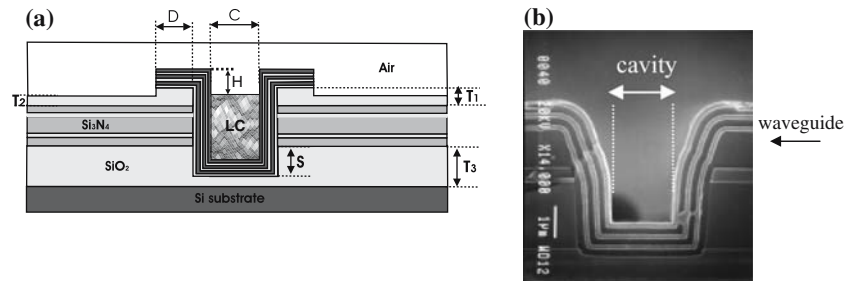


Fig. 2. (a) Cross section of the structure used to simulate the fabricated FP device. On odds with Fig. 1, there is a multilayer waveguide and a different height of the top cladding layer beneath the FP region than on the straight waveguide. The parameters used in the calculations are $D = 23 \mu\text{m}$, $C = 1.6/1.75 \mu\text{m}$, $H = 0 \mu\text{m}$, $S = 3 \mu\text{m}$, $T_1 = 1 \mu\text{m}$, $T_2 = 0.7 \mu\text{m}$, $T_3 = 3.1 \mu\text{m}$, $n_{\text{LC}} = 1.5$. (b) SEM cross section of the FP integrated within a waveguide.

The transmitted light at the exit of the waveguide both was imaged by a near field microscope objective matched to a variable zoom mounted on a high-performance infrared camera and controlled by beam analyzer software and was directed to a calibrated photodiode via a prism beam splitter.

The FP microcavity was infilled with Merck-K21 liquid crystal (K21 LCs). At 32°C K21 LCs show an isotropic behavior. At room temperature its refractive index is an average between the extraordinary and ordinary refractive index of nematic phase and results to be about 1.5. Hereafter we report the results for two different microcavities 1.6 and $1.75 \mu\text{m}$ long, nominally integrated in a monomode channel-waveguide. The transmitted spectrum was normalized to a straight reference waveguide transmission. No signature of FP resonances was observed in the empty devices. On the contrary, the devices infilled with K21 LC show typical resonances (Fig. 3 symbols). The shorter cavity has a transmission peak around 1320 nm while the longer cavity at 1467 nm. The observed shift (about 130 nm) is consistent with the difference of the cavity lengths. The structures were simulated with a commercial software¹ based on an eigenmode expansion (EME) method. A good agreement both for the spectral position and the linewidth was observed for the shorter cavity while only the spectral position was reproduced for the longer cavity (Fig. 3 lines).

5. Conclusion

Design, fabrication and initial tests of tunable optical switches integrated in silicon were performed. The preliminary results show that the devices

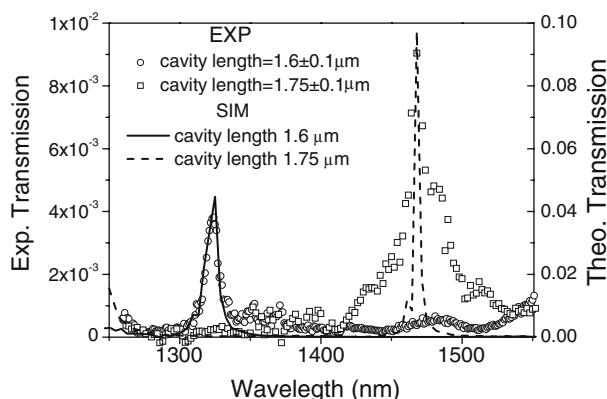


Fig. 3. TE polarized transmission spectrum for two different FP microcavities. The circle points/continuous line are the measured/simulated transmission spectrum of the device with a cavity length of $1.6 \mu\text{m}$. The squared points/dotted line are the measured/simulated transmission spectrum of the device with a nominal cavity length of $1.75 \mu\text{m}$.

are achievable even though an optimization is still needed. The integration of these switches in more complex optical integrated circuits could lead to dynamical optical routers fabricated within CMOS.

References

- Ctyroky, J. *J. Opt. Soc. Amer A*, **18** 435, 2001.
- Daldosso, N., M. Melchiorri, F. Riboli, F. Sbrana, L. Pavesi, G. Pucker, C. Kompocholis, M. Crivellari, P. Bellutti and A. Lui. *Materials Sci. Semiconductor Process* **7** 453, 2004.
- Melchiorri, M., N. Daldosso, F. Sbrana, L. Pavesi, G. Pucker, C. Kompocholis, P. Bellutti and A. Lui. *Appl. Phys. Lett.* **86** 121111, 2005.
- Mezzetti, A., G. Pucker, M. Crivellari, C. Kompocholis, P. Bellutti, A. Lui, N. Daldosso, F. Riboli, M. Saiani, Z. Gaburro and L. Pavesi. *Proc. SPIE*, **5357** 158, 2004.
- Palamaru, M. and P. Lalanne. *Appl. Phys. Lett.* **78**, 1466, 2001.
- Pavesi, L. and D. Lockwood. *Silicon Photonics Topics in Applied Physics*, Vol. 94. Springer-Verlag, Heidelberg, 2004.
- Pucker, G., A. Mezzetti, M. Crivellari, P. Bellutti, A. Lui, N. Daldosso and L. Pavesi. *J. Appl. Phys.* **96** 767, 2004.
- Riboli, F., N. Daldosso, G. Pucker, A. Lui and L. Pavesi. *IEEE J. Quantum Electron* **41** 1197, 2005.
- Sudbo, A.S. *Pure Appl. Optics* **2** 211, 1993a.
- Sudbo, A.S. *IEEE Phot. Tech. Lett.* **5** 342, 1993b.